

Identification of genes induced in proteoid roots of white lupin under nitrogen and phosphorus deprivation, with functional characterization of a formamidase

Mousumi Rath · Jay Salas · Bandita Parhy · Robert Norton ·
Himabindu Menakuru · Monika Sommerhalter · Greg Hatlstad ·
Jaimyoung Kwon · Deborah L. Allan · Carroll P. Vance · Claudia Uhde-Stone

Received: 11 November 2009 / Accepted: 30 March 2010 / Published online: 15 April 2010
© Springer Science+Business Media B.V. 2010

Abstract White lupin (*Lupinus albus* L.) is considered a model system for understanding plant acclimation to nutrient deficiency. It acclimates to phosphorus (P) and iron (Fe) deficiency by the development of short, densely clustered lateral roots called proteoid (or cluster) roots; proteoid-root development is further influenced by nitrogen (N) supply. In an effort to better understand proteoid root function under various

nutrient deficiencies, we used nylon filter arrays to analyze 2,102 expressed sequence tags (ESTs) from proteoid roots of P-deficient white lupin. These have been previously analyzed for up-regulation in –P proteoid roots, and were here analyzed for up-regulation in proteoid roots of N-deprived plants. We identified a total of 19 genes that displayed up-regulation in proteoid roots under both P and N

Responsible Editor: Michael Denis Cramer.

Mousumi Rath, Jay Salas, Bandita Parhy and Robert Norton contributed equally to this work.

Electronic supplementary material The online version of this article (doi:10.1007/s11104-010-0373-7) contains supplementary material, which is available to authorized users.

M. Rath · J. Salas · B. Parhy · R. Norton · H. Menakuru ·
C. Uhde-Stone (✉)
Department of Biological Sciences,
California State University, East Bay,
25800 Carlos Bee Blvd.,
Hayward, CA 94542, USA
e-mail: Claudia.stone@csueastbay.edu

R. Norton · J. Kwon
Department of Statistics,
California State University, East Bay,
Hayward, CA 94542, USA

M. Sommerhalter
Department of Chemistry & Biochemistry,
California State University, East Bay,
Hayward, CA 94542, USA

G. Hatlstad · C. P. Vance
Department of Agronomy and Plant Genetics,
University of Minnesota,
St Paul, MN 55108, USA

D. L. Allan
Department of Soil, Water, and Climate,
University of Minnesota,
1991 Upper Buford Circle,
St Paul, MN 55108, USA

C. P. Vance
USDA-ARS, Plant Science Research Unit,
1991 Upper Buford Circle,
St Paul, MN 55108, USA

deprivation. One of these genes showed homology to putative formamidases. The corresponding open reading frame was cloned, overexpressed in *E. coli*, and the encoded protein was purified; functional characterization of the recombinant protein confirmed formamidase activity. Though many homologues of bacterial and fungal formamidases have been identified in plants, to our knowledge, this is the first report of a functional characterization of a plant formamidase.

Keywords Proteoid roots · Cluster roots · Phosphorus deprivation · Nitrogen deprivation · Formamidase · Formate dehydrogenase · White lupin

Introduction

Nitrogen (N) and phosphorus (P) are the two most limiting nutrients for plant growth and development (Vance 2001). Loading of agricultural land with N and P fertilizers has devastating ecological consequences, such as eutrophication of salt- and fresh-water systems. P and iron (Fe) are often present in soils, but in forms unavailable for uptake by most crop plants (Marschner 1995). Improvement of nutrient acquisition and abiotic stress resistance in crops is considered critical for economic, humanitarian, and environmental reasons (Vance 2001; Welch and Graham 2004).

The well-characterized legume white lupin (*Lupinus albus* L.) has become an illuminating model system for understanding plant adaptations to nutrient deficiency, particularly to low P (Neumann and Martinoia 2002; Shane and Lambers 2005; Vance et al. 2003). White lupin's adaptation to P and Fe deficiency is a highly coordinated modification of root development and biochemistry, resulting in proteoid roots, which are densely clustered lateral roots, also called cluster roots (Dinkelaker et al. 1995; Hagström et al. 2001; Johnson et al. 1996b; Neumann and Römheld 1999; Shane and Lambers 2005). Transcript abundance of genes encoding phosphate transporters (Liu et al. 2001), acid phosphatase (Gilbert et al. 1999; Miller et al. 2001), or proteins related to organic acid synthesis (Massonneau et al. 2001; Peñaloza et al. 2002; Uhde-Stone et al. 2003) have been reported to be induced in proteoid roots of P-deficient white lupin. It has been shown that P deficiency increases proton extrusion by roots, and enhances the exudation of citrate and malate by white lupin plants (Dinkelaker

et al. 1995; Johnson et al. 1996a; Sas et al. 2001). Localized rhizosphere acidification and organic anion extrusion not only mobilizes P, but also other nutrients like Fe, manganese (Mn) and zinc (Zn) in the rhizosphere, and increases their rates of uptake (Lamont 2003; Lu and Zhang 1995; Marschner 1995). Dinkelaker et al. (1995) reported that low levels of N enhance formation of proteoid roots under P deficiency, while high N levels exhibit an inhibitory effect. In contrast, Sas et al. (2002) reported that addition of ammonium sources stimulate proteoid root formation and proton excretion under P deficiency. This apparent contradiction indicates a need for a better understanding of the influence of N on proteoid root formation and function. In addition to white lupin's exceptional ability to acquire P and Fe, it is also capable of symbiotic N fixation. In contrast to other legumes, white lupin's ability to fix N is less prone to inhibition by P deficiency (Schulze et al. 2006).

Not much is known about the gene network that allows white lupin to adapt well to a combination of nutrient stresses. Several microarray-based studies have assessed plant responses to nutrient stresses, such as N deficiency (Bi et al. 2007; Scheible et al. 2004), Fe deficiency (O'Rourke et al. 2009; Thimm et al. 2001) and P deficiency (Calderon-Vazquez et al. 2008; Misson et al. 2005; Peñaloza et al. 2002). These large-scale analyses of gene expression identified several hundred nutrient-responsive genes.

Nylon filter arrays have been used previously to analyze the expression of 2102 ESTs from white lupin proteoid roots to identify genes up-regulated under P-deprivation (Uhde-Stone et al. 2003). This approach has led to the identification of 35 genes that displayed significantly increased expression under P deprivation, including genes involved in carbon metabolism, secondary metabolism, P scavenging and remobilization, plant hormone metabolism, and signal transduction. Of special interest to us among these 35 genes were a putative formamidase and formate dehydrogenase, as both enzymes may function in the same pathway. Formamidases catalyze the conversion of formamide to formate and ammonia; formate dehydrogenases further oxidize formate to CO₂. Formate dehydrogenases have been previously reported to show induced expression under Fe deprivation in barley (Suzuki et al. 1998). Though many genes with homology to bacterial and fungal formamidases exist in plants, to our knowledge,

formamidase activity has not yet been confirmed for any of these plant homologues.

In the current study, the 2102 white lupin ESTs were used to analyze gene expression in proteoid roots of white lupin in response to N deprivation. The objectives of this research were 1) to use nylon filter arrays to identify a possible overlap of gene responses in proteoid roots under P and N deprivation, and 2) to functionally characterize formamidase, encoded by a gene that displayed induced transcript abundance in proteoid roots under, P, N, and Fe deprivation.

Materials and methods

Plant material and growth conditions

Lupinus albus L. var Ultra plants were grown in a growth chamber at 20/15°C and 16-/8-h day/night cycles, 300 $\mu\text{mol photons m}^{-2} \text{s}^{-1}$ at shoot height, and 70% relative humidity. Plants were grown in silica sand culture watered with Hoagland nutrient solution, which was replenished every other day, as described previously (Johnson et al. 1996b). The complete nutrient solution (control) consisted of 3.0 mM KNO_3 , 2.5 mM $\text{Ca}(\text{NO}_3)_2$, 0.5 mM $\text{Ca}(\text{H}_2\text{PO}_4)_2$, 1.0 mM MgSO_4 , 12.0 μM Fe (as FeEDTA), 4.0 μM MnCl_2 , 22.0 μM H_3BO_3 , 0.4 μM ZnSO_4 , 0.05 μM NaMoO_4 , and 1.6 μM CuSO_4 . N deprivation was defined by the presence of KCl (3 mM) and CaSO_4 (0.5 mM) substituting for 3 mM KNO_3 and 2.5 mM $\text{Ca}(\text{NO}_3)_2$. P deprivation was imposed by the presence of 0.5 mM CaSO_4 , substituting for 0.5 mM $\text{Ca}(\text{H}_2\text{PO}_4)_2$ in the nutrient solution. Fe deprivation was imposed by withholding Fe-EDTA from the nutrient solution. For validation experiments, white lupin was grown hydroponically in a growth chamber using the same settings and nutrient solutions as described above for silica sand culture. About four plants per container were grown in 1 L aerated nutrient solution, which was replenished every two days. To reduce any effect of diurnal changes on gene expression, all samples were collected during the middle of the day.

Nylon filter array spotting and hybridization

Nylon filter array spotting, using an automated Q-bot spotting protocol, and hybridization of arrays

were performed as previously described (Uhde-Stone et al. 2003). The nylon filter arrays included two independent biological replicates for each experimental condition. In addition, each EST was spotted twice per filter, resulting in a total number of 4 replicates per EST and condition.

Statistical analysis for the identification of differentially expressed genes

For nylon filter array analysis, background noise was subtracted from individual filter spot intensities using Array Pro Analyzer software (Media Cybernetics; Carlsbad, CA, USA). Data were normalized (Dudoit et al. 2002; Ness 2007; Watson et al. 2007) using R statistical software (<http://www.r-project.org/>). The data were centered about independent array means (Element Intensity—Array Mean Intensity = Array Mean Normalized Intensity (AMNI)). Next these array-normalized intensities were corrected for gene-specific variation attributable to the replicate number (AMNI—Replicate Median = Replicate Median Normalized AMNI (RMNI)). Analysis of Variance (ANOVA) tests were performed on the RMNI data comparing control with both N and Fe deficiency to determine statistical significance of differential gene expression. A one-way ANOVA in R was completed utilizing a Benjamini-Hochberg method to further reduce the chance of a Type I Error (α). For genes discussed in this paper, a conclusion of statistical significance for array data compared by ANOVA testing means that significant variation can be found between the treatment groups, and this variation is attributable to the different nutrient conditions. After subtracting the array and replicate specific values, a small constant was added to all expression values (as applied in Orzack and Gladstone 1994) to ensure positive values (RMNI + 100 = Constant Added Normalized Intensities (CANI)). Ratios of gene expression between nutrient-stress conditions were calculated from the Constant Added Normalized Intensities (CANI).

RNA preparation

Total RNA was extracted using an RNeasy Mini kit (Qiagen, Valencia, CA, USA). To eliminate genomic DNA contamination in RNA, the RNA was treated with Turbo-DNase followed by DNase

inactivation, as per the manufacturer's instructions (Ambion, Foster City, CA, USA). Quantification of RNA was done using the RiboGreen (Invitrogen, Carlsbad, CA, USA) protocol for the Nanodrop ND-3300 Fluorospectrometer (Nanodrop, Wilmington, Delaware, USA), following the manufacturer's instructions.

Reverse-transcription quantitative PCR (RT-qPCR)

SuperScript III Platinum Two-Step qRT-PCR Kit with SYBR Green (Invitrogen) was used for the RT-qPCR reaction. First strand cDNA was synthesized according to manufacturer's instructions, using premixed random hexamer and poly-d(T) primers supplied with the kit. A no-Reverse Transcriptase (no-RT) control reaction was included to control for genomic DNA contamination.

Quantitative (real-time) PCR was performed on the Opticon™2 system (MJ research, San Francisco, CA, USA). The primer pairs used are listed in Table 1. Four reference genes were analyzed using geNORM (Vandesompele et al. 2002), namely gamma-tubulin, cyclophilin, aquaporin, and ubiquitin; ubiquitin was chosen as the main reference gene for RT-qPCR analysis. As some ubiquitins and aquaporins showed high differential expression in

the array, L#1223 (40S ribosomal protein S8), a gene with fairly even expression level throughout the array, was used as additional reference gene. Delta amplification efficiency between target and reference genes was <0.2 for each primer pair.

For quantitative PCR, Platinum® SYBR® Green qPCR SuperMix-UDG (Invitrogen) was used following manufacturer's instructions and the following protocol: 50°C 2 min, denaturation at 94°C for 2 min, amplification and quantification for 40 cycles of 94°C for 40 s, 60°C for 45 s, 72°C for 45 s with a single fluorescence measurement, followed by melting curve determination (50–95°C) with a heating rate of 0.5°C per 0.5 s and a continuous fluorescence measurement.

All samples were amplified in triplicate. Standard curves were determined for sample and reference genes. Fold changes, normalized to the reference genes, and corrections for differences in amplification efficiencies, were determined by using the Q-Gen program (Simon 2003).

Cloning and expression of recombinant formamidase

For cloning and expression of recombinant formamidase, the champion pET200/D-TOPO Expression kit (Invitrogen) was used to generate an N-terminal His-tag,

Table 1 Primer pairs of target and reference genes used for RT-qPCR

Gene	Primer sequence	Amplicon size
Sucrose synthase	Forward: TGACACGAGGGGTGCTTTT Reverse: ATTGGAAGTGGCGAAGGTT	103 bp
GAPDH	Forward: CGATCCTTTCATCACCCTG Reverse: CTCCTCAGGGTTCCTGTGTC	157 bp
Formate dehydrogenase	Forward: CCGTTCGATCCATCACTTCT Reverse: GATTCCTCAACAGAGCCTA	152 bp
Formamidase	Forward: TCACCAGTGCTGAGATTTGC Reverse: AAAAAGGCACTG CTGAATGG	157 bp
L#315 "unknown"	Forward: TGGGAAAACGATGCCTATCT Reverse: CCTTGGCTTGGACAGAGTG	158 bp
Ubiquitin ^a	Forward: TCTTTGTGAAGACCCTCACC Reverse: CTGCTGGTCCGGAGGAATG	400 bp
40 S ribosomal protein S8 ^a	Forward: AGGGCATTGAGATTGGACAC Reverse: GAGCAGCATCAA CCTGAAC	157 bp
Aquaporin ^b	Forward: CAGCACCAGAAGTTTCCAT Reverse: CTTGCAGGTTTGACCCAGAT	152 bp
Gamma tubulin ^b	Forward: CTCGAACATGGAATCAGCAA Reverse: AATAACCCTCGGCTCCAAGT	144 bp
Cyclophilin ^b	Forward: AATGAACGGTGAGGGACAT Reverse: GACACAGATCAGAGCCACCA	139 bp

^aReference genes used in this study

^bReference genes tested with geNorm, but not used in this study for normalization

following manufacturer's instructions. The kit is designed for directional insertion of blunt end PCR products into the vector and high levels of inducible protein production. Amplification was performed with the proofreading Pfu DNA polymerase (Stratagene, La Jolla, CA, USA) to generate error-free blunt end PCR products. The primers for amplification of the formamidase ORF were: CACC ATG GCA CCA CAA ACT CCA AAA (forward), and TCA TTG TGT AGC ACT AAG ATT C (reverse). Transformants were analyzed by colony PCR, and by *NheI* and *SacI* double digest to confirm the presence of the insert in the plasmid pET200. Sequencing was used to confirm error-free amplification and correct insertion into the vector.

Protein expression and purification

Expression of recombinant formamidase in BL21 Star™ (DE3) *E. coli* was done following the Invitrogen protocol. In short, pET200/D-TOPO plasmid was used for transformation of BL21 Star™ (DE3) One Shot® cells. Transformed BL21 Star™ (DE3) cells were grown in LB medium, and expression of formamidase was induced with IPTG (final concentration of 1 mM). Cultures without IPTG induction with (for repression of protein expression) and without added glucose were grown as controls. Cultures were incubated at 37°C with shaking for 4 h.

The recombinant formamidase protein was isolated via its N-terminal His-tag, using the MagneHis™ Protein purification system (Promega, Madison, WI, USA), following manufacturer's instructions. This kit contains all reagents needed for cell lysis, protein binding, washing and elution. The concentration of purified protein was determined via Bradford assay (Bradford 1976).

Total protein for crude extract measurements was isolated using the P-PER protein isolation kit (Pierce, Rockford, IL, USA). Proteoid roots from white lupin grown without N were collected 21 DAE (days after emergence). About 500 mg of fresh tissue were lysed in a mesh bag; extracts were prepared according to manufacturer's instructions with the following modification: 50 µl protease inhibitor cocktail (EDTA-free; Pierce, Rockford, IL) and 0.2 mM PMSF (prepared freshly on the day of extraction) were added. The nuclear protein extract was then stored at -70°C.

Growth of *E. coli* overexpressing LaFmd on formamide as only N-source

M9 minimal medium (Sambrook and Russell 2001) was used to test the ability of BL21 Star™ (DE3) cells overexpressing recombinant LaFmd to use formamide as only N source. IPTG-induced BL21 Star™ (DE3) overexpressing LaFmd or vector control (inserted *LacZ* gene; provided with pT200 kit, Invitrogen) were plated on M9 medium containing 50 mg/ml kanamycin and either 0.1% NH₄Cl (regular M9 medium) or 0.1% formamide (modified M9 medium) as only N-source. Colony size was analyzed visually after 2 days of incubation at 37°C.

Formamidase enzyme assay

An enzyme assay for formamidase activity was used as described by (Skouloubris et al. 1997); the assay was performed in the dark to avoid a rapid photochemical side reaction that interferes with the assay (Gravitz and Gleye 1975). In essence, 10–50 µl of purified protein or 50 µl crude extract were added to 200 µl formamide in substrate solution of different concentrations, ranging from 1 mM to 600 mM, in PEB (PEB = 100 mM Phosphate buffer pH 7.4, 10 mM EDTA). The reaction mixture was incubated at 30°C for 30 min. 400 µl of phenol-nitroprusside (Sigma, St. Louis, MO, USA) and 400 µl of alkaline hypochlorite solution (Sigma, St. Louis, MO) were added to the sample. Samples were incubated at 50°C for 6 min, and absorbance was measured at 625 nm. The amount of ammonia was determined with the help of a standard curve (Skouloubris et al. 1997). For the standard curve, known amounts of NH₄Cl were added to hypochlorite solution. The standard curve samples were treated as the reaction samples, with the exception that incubation at 30°C was shortened to 10 min, as dissociation did not change further with prolonged incubation.

Characterization of formamidase

Enzyme activity was measured at different concentrations of formamide, propionamide, and nicotinamide, respectively, and the V_{max} and K_m were calculated, using the program EnzFitter (Biosoft, Cambridge, United Kingdom). To determine the temperature and pH optima of formamidase, the

enzyme was mixed with formamide in saturated substrate concentration and incubated at various temperatures and pH, respectively.

Results

To assess gene expression in proteoid roots of N-deprived white lupin, plants were grown in silica sand culture watered with either N-lacking (–N) or complete (+N) nutrient solution. Three weeks after emergence, fully developed proteoid roots had formed and were collected. The number and appearance of proteoid roots under N deprivation was similar to those formed under P deprivation, however, it took 21 DAE (days after emergence) to form fully developed proteoid roots under N deprivation, compared to only 14 DAE under P deprivation.

Nylon filter arrays of 2102 white lupin ESTs (spotted in duplicate) derived from –P proteoid roots (Uhde-Stone et al. 2003) were hybridized with 1st strand cDNA from proteoid roots of N-deficient plants and nutrient-sufficient control plants in two biologically independent replications. Data were normalized and ratios of transcript abundance between different conditions were calculated as described in Materials and Methods. The selection criteria for differential transcript abundance were ratios of ≥ 2 or ≤ 0.5 , and $\alpha=0.05$; α is the significance level that corresponds to a p-value of less than 5%. To reduce the number of false positives, a contig was only included if at least two thirds (66%) of the member fragments matched the selection criteria, and/or significant up-regulation was confirmed by RT-qPCR (reverse-transcription quantitative PCR).

Of a unigene set of 1448, we identified 359 unigenes (about 25%), grouped in 77 contigs and 282 singletons, that displayed at least 2-fold increase of expression in proteoid roots of N-deficient plants, compared to proteoid roots of nutrient-sufficient controls (supplementary Table s1). 27 unigenes (1.8%) displayed a 2-fold or greater decrease in transcript abundance (supplementary Table s2). A complete list of normalized array data (Table s3) and raw data (Table s4) is shown in supplementary materials. Of the 359 unigenes that displayed increased expression, 19 have been previously identified as induced in proteoid roots of P-deficient white lupin (Table 2).

Confirmation of expression pattern for selected ESTs by RT-qPCR

For confirmation of expression pattern, white lupin plants were grown hydroponically for 3 weeks in either complete nutrient solution, or in nutrient solution lacking P, N or Fe, respectively. Fully developed proteoid roots were collected; nutrient-sufficient lupin plants formed proteoid roots that were similar in appearance to those formed under P deprivation, though they were fewer in numbers. RT-qPCR was performed and confirmed up-regulation in 4 out of 5 ESTs (Table 3). Increased expression of Glyceraldehyde 3-phosphate dehydrogenase (GAPDH) was not confirmed, though GAPDH displayed a slight increase of expression (1.5), this was below the cut-off value of 2. Genes with homology to formamidase and formate dehydrogenase, respectively, displayed induction in proteoid roots under P, N, and Fe-deprivation. Normal roots (defined as roots sections that did not show dense root clusters) also displayed an increase in transcript abundance under the tested nutrient deficiencies, except for formamidase under Fe deprivation (Table 4). No-template control served as negative control, and no-RT controls confirmed the absence of genomic DNA contamination.

Comparative analysis

As very little is known about the function of formamidases in plants, we decided to further analyze the putative formamidase gene. The complete cDNA clones corresponding to two of the four redundant formamidase ESTs (L#41, L#109; Uhde-Stone et al. 2003) were sequenced (GenBank accession # FJ617192). The most likely open reading frame (ORF) of the cDNA sequence was identified using the program “Translate” (<http://www.expasy.ch/tools/dna.html>). The predicted ORF sequence contained 452 amino acids, resulting in a predicted protein of 49.774 kDa; a BlastP search showed that this open reading frame displayed homology to other formamidases.

High sequence similarity was found with a number of plant proteins, including two putative formamidases from *Arabidopsis* (Table 5). The closest sequence similarity to a functionally confirmed formamidase (FmdA of *Methylophilus methylotrophus*) was 68% (49% identity; Table 5). The phylogram in Fig. 1 displays the relationship of LaFmd and selected homologues.

Table 2 ESTs that show an at least 2-fold induction in proteoid roots under N deprivation, and have been previously identified as 2-fold or more induced in -P proteoid roots, compared to +P normal roots (Uhde-Stone et al. 2003)

Identifier/ GenBank accession	Annotation ^a	E-value	Possible function	Ratio proteoid root -N/+N	p-value
L#470/ CA410203	Glyceraldehyde-3P-dehydrogenase (NAD)	1E-28	Glycolysis	15.2	2E-7
L#471/ CA410204	LaMATE	0	Transport of small organic molecules	10.6	0.008
L#350/ CA410092	Fructose-biphosphate aldolase, cytoplasmic	5E-44	Glycolysis	9.9	2E-5
L#315/ CA410054	Unknown	2E-11		5.9	2E-5
L#626/ CA410354	Malate dehydrogenase	9E-59	Organic acid metabolism	5.1	8E-7
L#374/ CA410116	Cytochrome P450/ ferrulate-5-hydroxylase	5E-28	Flavonoid biosynthesis	5.1	2E-5
L#33/ CA410080	Phosphoglycerate kinase, cytosolic	3E-33	Glycolysis	4.9	6E-7
E#711/CA411412	Unknown	6E-58		4.1	6E-5
L#103/ CA840666	Phosphofructokinase family protein	5E-14	Glycolysis	3.8	9E-4
L#197/ CA409931	Sucrose synthase	8E-55	Sugar metabolism; signaling	3.3	5E-4
E#81/CA410808	Putative senescence-associated protein	2E-26	Unknown	3.3	2E-4
L#65/ CA410389	Unknown	9E-14		2.7	8E-4
L#723/ CA410456	Xyloglucan endo-1, 4-beta-D-glucanase	1E-31	Root hair development	2.7	4E-4
L#771/ CA410506	Malate synthase, glyoxysomal	1E-38	Glyoxysomal pathway	2.4	3E-3
L#1098/ CA409560	Triosephosphate isomerase cytosolic	4E-56	Glycolysis	2.3	1E-3
E#241/CA410959	2,3-bisphosphoglycerate-independent phosphoglycerate mutase	1E-34	Glycolysis	2.9	6E-5
L#41/ CA410157	Formamidase-like protein	1E-81	Conversion of formamide	2.3	4E-4
L#218/ CA409954	Formate dehydrogenase, NAD	8E-55	Anaerobic metabolism	2.1	6E-3
L#210/ CA409946	Calcium binding protein	6E-21	Signal transduction	2.0	1E-3

^aBlastX search October 2009

A Blastn search with the LaFmd sequence against the *Arabidopsis* genome at TAIR (www.arabidopsis.org) and the rice genome at Rice Genome Annotation (<http://rice.plantbiology.msu.edu>), respectively, identified a total of 2 formamidase homologues in the *Arabidopsis* genome located in tandem (AT4G37550, AT4G37560), both annotated as putative formamidases, and 2 homologues in the *Oryza sativa* genome (Os01g076490, annotated as putative formamidase, and LOC_Os01g55950, annotated as putative acetamidase).

As LaFmd displayed high sequence similarity to both putative formamidases in *Arabidopsis*, we assessed the expression of both *Arabidopsis* homologues via elec-

tronic northern, using Geneinvestigator (<https://www.geneinvestigator.ethz.ch/gvs/index.jsp>). *Arabidopsis* homologue At4g37550 displayed 3-fold higher, At4g37560 15-fold higher transcript abundance in leaves than in roots, and both homologues did not show any induction under P or N deprivation. We were further interested in assessing formamidase homologues in *Medicago truncatula*, as this legume is more closely related to white lupin. We searched the *M. truncatula* gene index (MtGI; <http://compbio.dfci.harvard.edu/tgi>) for ESTs with homology to LaFmd, and identified a tentative consensus (TC123775) of 29 ESTs (84% identity, 92% similarity). An electronic northern using the expression report tool of MtGI revealed relatively

Table 3 RT-qPCR validation of selected ESTs that showed at least 2-fold induction in proteoid roots under $-N$ (this study) and $-P$ (Uhde-Stone et al. 2003)

Identifier	Annotation	Proteoid root fold change $-N^1$	Proteoid root fold change $-Fe^1$
L#197	Sucrose synthase	3.4±0.8	4±0.3
L#470	Glyceraldehyde-3 P dehydrogenase	1.5±0.1	1.7±0.2
L#41	Formamidase	72.3±7.3	39.8±1.8
L#218	Formate dehydrogenase	35±4.4	32±0.5
L#315	Unknown	3.2±0.7	2.7±0.1

¹ Shown are mean-normalized expressions of three experimental replications ± SEM (standard error of the mean) of a representative from at least two biological replications

low transcript abundance of the corresponding gene in P-starved roots (0.04% of total library) and leaves (0.01% of total library). Highest expression was found in virus-infected leaves and aphid-infected stems (each representing 0.06% of total library).

Computational analysis using the tool WoLF PSORT (Horton et al. 2007) indicated that *LaFmd* and its close homologue in *Vitis vinifera* (CAN78133.1) are likely localized in the cytosol. WoLF PSORT analysis was inconclusive in regard to cellular localization prediction of the Arabidopsis, *M. truncatula* and *O. sativa* formamidase homologues. ChloroP (Emanuelsson et al. 1999) predicted no chloroplast signal for any of the analyzed plant formamidase homologues. MitoProt II (Claros and Vincens 1996) predicted putative mitochondrial signal peptides for the *M. truncatula* homologue, as well as for one of the two Arabidopsis homologues (At4G37550).

Expression and purification of recombinant formamidase

Computational analysis had identified many formamidase homologues in plants, but a literature search revealed no evidence for functional characterization of any plant formamidase. In order to confirm formamidase activity of LaFmd, the LaFmd ORF was amplified from the cDNA clone corresponding to EST L#109 (Uhde-Stone et al. 2003), cloned into an expression vector containing an N-terminal His tag (pET200/D-TOPO), and overexpressed in *E. coli*. The purified formamidase was detected on an SDS-PAGE after

induction with IPTG, while no or only minimal expression was seen in the uninduced sample (Fig. 2). The SDS-PAGE indicated a molecular weight of the recombinant formamidase (including the His-tag) of about 52 kDa.

Growth of *E. coli* overexpressing LaFmd on formamide as only N-source

E. coli overexpressing recombinant LaFmd were grown on 0.1% formamide as only N source as an initial test for formamidase activity. *E. coli* strain BL21 Star™ (DE3) overexpressing LaFmd was able to grow on selective medium containing formamide as only N source, while *E. coli* BL21 Star™ carrying a vector control (expressing *lacZ* instead of LaFmd) displayed only marginal growth (Fig. 3). As control, both strains were grown on minimal medium containing 0.1% NH₄Cl as only N source, resulting in similar colony size (data not shown).

Formamidase activity assay

Formamidase activity of LaFmd was further assessed using an ammonium assay (Skouloubris et al. 1997); enzyme characteristics are shown in Fig. 4. A K_m of 71±15 mM was determined for the substrate formamide for the recombinant formamidase (Fig. 4a, b). To confirm that this is truly the K_m of native LaFmd, and not an artifact of heterologous expression of a recombinant protein, we tested formamidase activity in protein crude extract from proteoid roots of N-deprived white lupin. These measurements indicate a

Table 4 Assessment of relative transcript abundance by RT-qPCR analysis of formamidase and formate dehydrogenase in $-P$ proteoid roots, compared to $+P$ proteoid roots, and in $-P$, $-N$ and $-Fe$ normal roots, compared to nutrient-sufficient normal roots

Annotation	Proteoid root fold change $-P/+P^1$	Normal root fold change $-P/+P^1$	Normal root fold change $-N/+N^1$	Normal root fold change $-Fe/+Fe^1$
Formamidase	19.7±0.5	2.6±0.6	6±0.5	1±0.1
Formate dehydrogenase	3±2.5	3.2±0.5	7±1	2.5±0.1

¹ Shown are averages of three experimental replications ± SEM of a representative from at least two biological replications

Table 5 Selected homologues of LaFmd

GenBank accession #	Sequence identity/ similarity	Annotation	Organism
CAN78133.1	88%/95%	Hypothetical protein	<i>Vitis vinifera</i> (grapevine)
NP_568029.1	82%/90%	Formamidase, putative	<i>Arabidopsis</i> At4G37560
ACF87318.1	79%/90%	Unknown	<i>Zea mays</i>
NP_001044346.1	79%/90%	–	<i>Oryza sativa</i> Os01g0764900
NP_568028.1	81%/90%	Formamidase, putative	<i>Arabidopsis</i> AT4G37550
ABK21753	73%/83%	Unknown	<i>Picea sitchensis</i> (Sitka spruce)
XP_001699344.1	75%/84%	Formamidase	<i>Chlamydomonas reinhardtii</i> (green alga)
XP_001775936.1	73%/85%	Predicted protein	<i>Physcomitrella patens</i> (moss)
YP_001520245.1	58%/73%	Formamidase	<i>Acaryochloris marina</i> (Cyanobacterium)
YP_475820.1	58%/73%	Acetamidase/formamidase family protein	<i>Synechococcus</i> sp. (Cyanobacterium)
YP_001832114.1	55%/69%	Formamidase	<i>Beijerinckia indica</i> (Proteobacterium)
sp Q50228 FMDA_METME	49%/68%	Formamidase FmdA (Silman et al. 1991; Wyborn et al. 1996)	<i>Methylophilus methylotrophus</i> (Proteobacterium)
AFUA_2G02020	51%/61%	Formamidase FmdS	<i>Aspergillus fumigatus</i> (Fungus)

K_m of 56 ± 7 mM (Fig. 4b, c), which falls within the same range as that determined for the recombinant enzyme. Two additional potential substrates, propionamide and nicotinamide were tested, and displayed K_m values of about 120 mM for propionamide, and no activity for nicotinamide. The enzyme activity using formamide as substrate was measured at different temperatures (namely 20°C, 30°C, 40°C, 50°C, 60°C and 70°C). The optimum temperature was identified to be in the 30°C to 50°C range for recombinant formamidase (Fig. 4e). To confirm this result and to narrow down the optimal temperature range, total protein crude extract was tested at 35°C, 40°C, 45°C (data not shown) and displayed optimal formamidase activity between 35°C and 45°C. The formamidase activity was further tested at different pH, namely pH 6, 7, 8 and 9. The enzyme was found to be active in the pH 6–9 range; the maximum enzyme activity was obtained between pH 6 and pH 8 (Fig. 4f).

Discussion

In this report, we have advanced our understanding of white lupin proteoid root responses to nutrient deficiencies by (a) identifying genes induced in

proteoid roots under both –P and –N deprivation, and b) cloning and overexpression of the *LaFmd* gene, which displayed increased transcript abundance in proteoid roots under –N, –P, and –Fe, and purification and functional characterization of the encoded protein.

The number of genes showing increased expression in this study is much higher than what has been found previously in a microarray study of chronic N-deficient *Arabidopsis* by Bi et al. (2007), who identified 271 genes (about 1%) showing increased and 190 genes (about 0.7%) showing decreased expression, compared to nutrient-sufficient plants. The higher number of genes displaying increased expression, and the relatively low number of genes showing reduced expression in our study may be explained by the focus of this study on proteoid roots, and the source of cDNA used as probes (spotted on the arrays), as these were isolated from –P proteoid roots, and were thus enriched for genes with increased expression in nutrient-stressed proteoid roots.

The LaMATE gene was found among the 10 most highly expressed unigenes in this study. As LaMATE has been previously identified as being induced in proteoid roots under various nutrient deficiencies (Uhde-Stone et al. 2005), LaMATE can be regarded

Phylogenetic tree

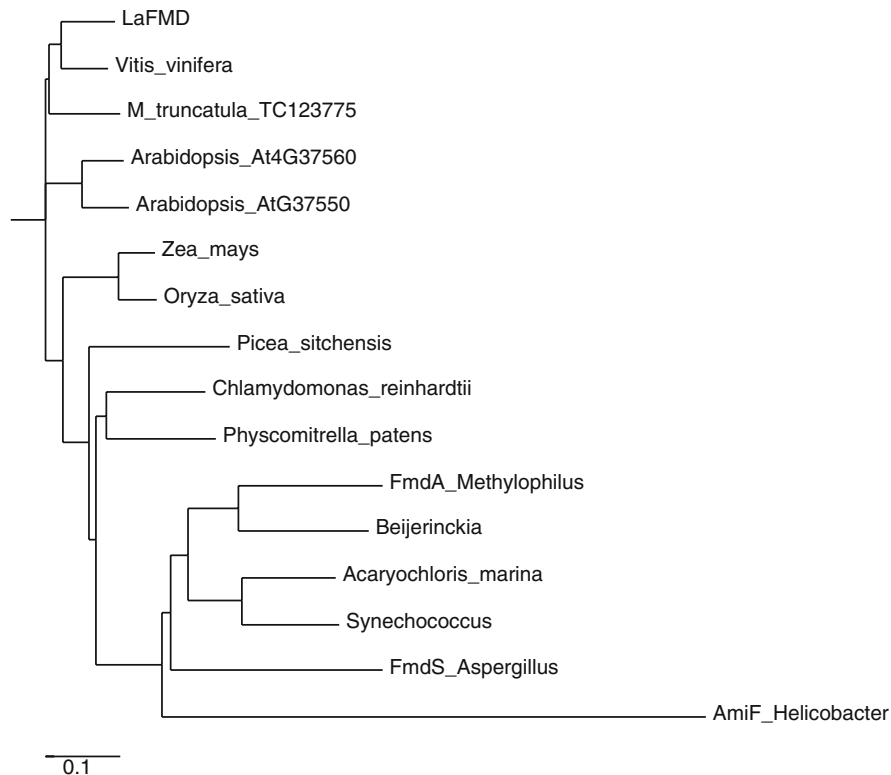


Fig. 1 Phylogram of deduced amino-acid sequences from selected formamidase genes and functionally uncharacterized homologues. The phylogram was derived using the CLUSTALW program at the European Bioinformatics Institute (EBI; <http://www.ebi.ac.uk/clustalw>)

as a positive control to assess if the nylon filter array detects differential transcript abundance. 9 out of 10 members of the LaMATE contig displayed relative expression ratios above 2, and thus confirmed the array analysis. The fact that one member of the LaMATE contig was not revealed by the array as having differential transcript abundance, however,

indicates the existence of false negatives. This could be due to low amplification of individual cDNAs or cDNA degradation before or during spotting.

We compared the 359 unigenes identified as induced under $-N$ with ESTs previously identified as induced in

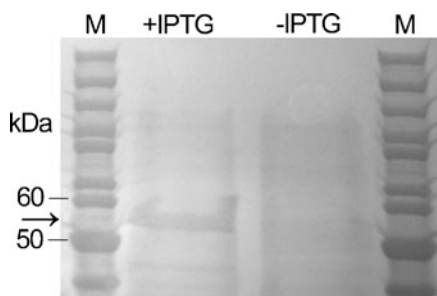


Fig. 2 SDS PAGE displaying a protein of correct size (about ~52 kD) after IPTG induction. In contrast, no purified protein was obtained from uninduced culture ($-IPTG$)



Fig. 3 *E.coli* BL21 StarTM (DE3) cells overexpressing LaFmd displayed growth, visible as colonies (left), compared to *E.coli* BL21 StarTM (DE3) control, expressing the *lacZ* gene (right), when grown on M9 minimal medium with formamide as only N source

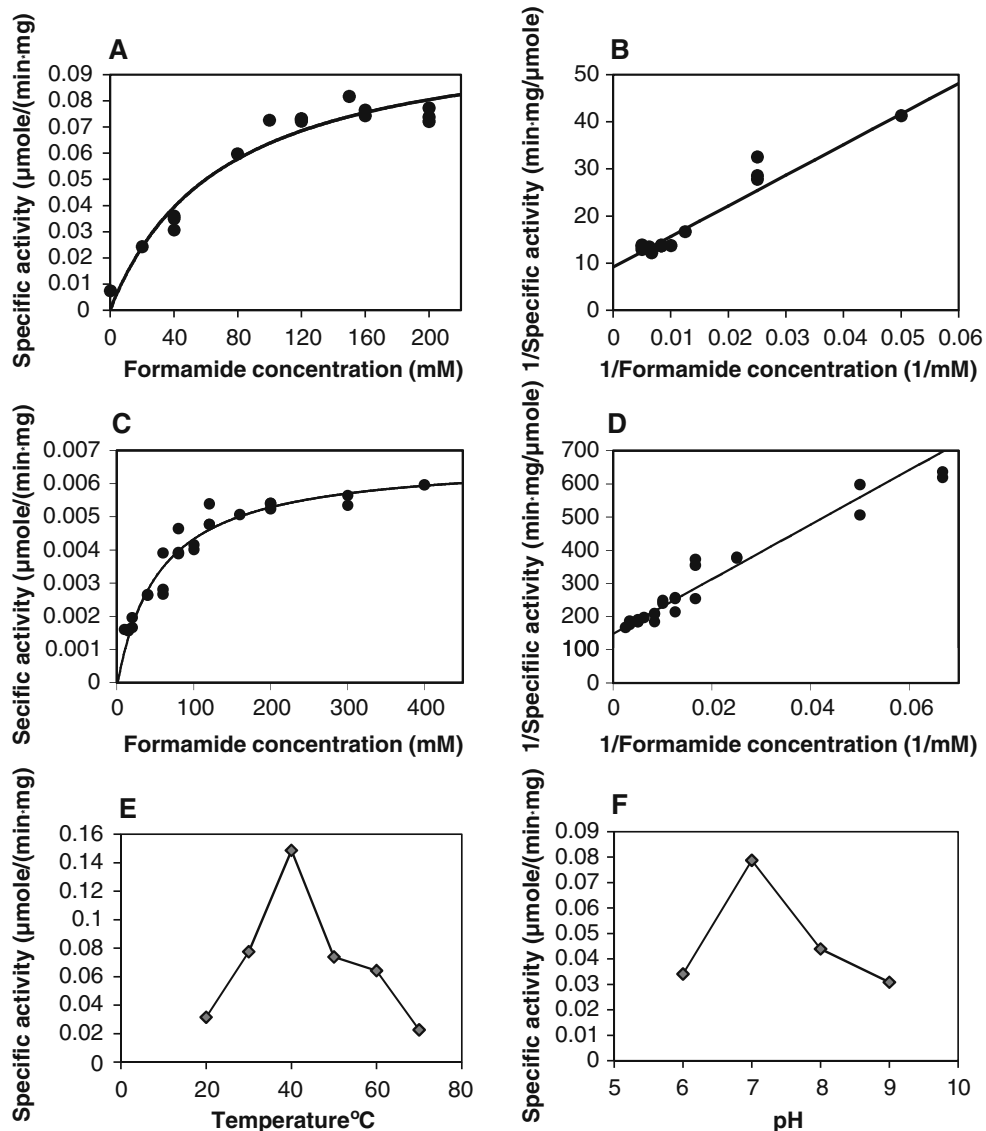


Fig. 4 Enzyme kinetics of recombinant LaFmd expressed in *E. coli* (**a**, **b**) and in total protein crude extract of *L. albus* proteoid roots (**c**, **d**), calculated using the program EnzFitter. **a**–**d** display results of 3 independent replications **e**. Determination of

temperature optimum and **f**. pH optimum for recombinant LaFmd. Formamide was used as substrate (**a**–**f**). **E** and **F** show representative measurements of 2 independent replications

proteoid roots of P deficient white lupin (Uhde-Stone et al. 2003). 19 out of the 35 unigenes (54%) previously identified as induced in $-P$ proteoid roots were also induced in proteoid roots under N deprivation. This large overlap of genes differentially expressed in proteoid roots under N and P deprivation indicates that a large number of genes involved in proteoid root function may not be specific to a particular nutrient stress. This conclusion is further supported by the finding that 4 out of 5 genes analyzed by RT-qPCR

displayed increased expression in proteoid roots not only under $-N$, but also under $-Fe$ (Table 3).

Based on homology comparison, 9/19 genes (47%) that displayed increased expression in proteoid roots of both $-N$ and $-P$ plants are involved in carbon metabolism. The finding that sucrose synthase displayed an increase in expression in proteoid roots under N, P and Fe deprivation is of special interest, as sugar signaling has been shown to mediate plant responses to $-N$, $-P$, and possibly other biotic stresses

(Hammond and White 2008; Liu et al. 2005; Price et al. 2004), and has been demonstrated to be involved in the formation of proteoid roots (Zhou et al. 2008). In addition, several enzymes involved in glycolysis displayed increased expression under both N and P stress, possibly as a result of the higher sugar allocation to nutrient-stressed roots, and the organic acid excretion observed in proteoid roots in response to nutrient deficiencies. Other genes that may have more specific functions in P_i acquisition and uptake, such as acid phosphatases and P_i transporter, were only induced in proteoid roots of P-deficient, but not of N-deprived plants. Interestingly, genes with homology to formamidase and formate dehydrogenase, two enzymes possibly acting in the same metabolic pathway, were both induced in proteoid roots under P, N and Fe deprivation.

The enzymatic activity of formamidases has been characterized in bacteria and fungi, but (to our knowledge) not in plants. Thus, we focused on the characterization of formamidase (LaFmd). Computational analysis revealed highest expression of formamidase homologues in *Arabidopsis* and *M. truncatula* in pathogen-infected shoots, while LaFmd expression in leaves of white lupin, has previously been shown to be below detection (Uhde-Stone et al. 2003). These strikingly different transcript accumulation patterns in *M. truncatula* and *Arabidopsis*, compared to LaFmd, may indicate different roles of the corresponding proteins.

SDS-PAGE indicated a molecular weight of about 52 kDa (including the His-tag), which correlates to the predicted molecular weight of ~49.8 kDa (Expasy) of the native protein. In comparison, molecular weights of formamidases in other species are 44.5 kDa for FmdA in *Methylophilus metophilus* (Wyborn et al. 1996), 44 kDa for FmdS in *Aspergillus nidulans* (Hynes 1975) and ~37 kDa for AmiF in *Helicobacter pylori* (Skouloubris et al. 2001). Compared to most fungal and bacterial formamidases, the predicted molecular weights of putative formamidases in plants, algae and cyanobacteria are generally larger, due to additional sequences at the C-terminus.

LaFmd had a high K_m of about 71 ± 15 mM measured for the recombinant protein. Kinetic measurements using protein crude extract resulted in a K_m of within the same range (56 ± 7 mM), indicating that the high K_m value is not an artifact caused by the His-tag, or the expression in a heterologous system. In comparison, the K_m value

for the substrate formamide was 2.1 mM for FmdF in *M. metophilus* (Silman et al. 1991), and 32 mM for AmiF in *Helicobacter pylori* (Skouloubris et al. 2001). The biochemical properties of similar amidases have been described in a number of bacteria (Fournand and Arnaud 2001), including *Pseudomonas*, *Rhodococcus*, *Mycobacterium*, *Bacillus* and *Brevibacterium*, and most expressed much higher activities with short-chain aliphatic amides than with formamide. Thus, we tested the short-chain amide propionamide as possible substrate for LaFmd, however, this resulted in an even higher K_m of 120 mM, indicating that short-chain amides are not a likely substrate. Of course, the possibility remains that LaFmd prefers yet another substrate that we have not identified. Despite the high K_m , the fact that *E. coli* overexpressing LaFmd gained the ability to grow on formamide as only N-source confirmed formamidase activity of LaFmd.

Formamidase catalyzes the conversion of formamide to formate and ammonia. The up-regulation of the formamidase gene under -N deprivation suggests that formamidase is involved in providing an alternative source of N in form of ammonia cleaved off from formamide and possibly other substrates. Formamide has been shown to be a degradation product of both histidine and cyanide in various microorganisms (Ferber et al. 1988; Kunz et al. 1994). It has been speculated that formamidase may play a role in detoxification of cyanides in plants (Fraser et al. 2001).

The up-regulation of LaFmd under P and Fe deprivation is difficult to explain. Formamidase activity produces formate, a major C1 unit source (Cossins and Chen 1997). Formate can be further metabolized by the enzyme formate dehydrogenase. Interestingly, we also identified a putative formate dehydrogenase (FDH) as up-regulated in proteoid roots under P, N, and Fe deprivation. FDH catalyzes oxidation of formate to CO_2 , and is thought to play a role in anaerobic respiration (Suzuki et al. 1998). Fe deprivation, a stress that mimics anaerobiosis due to the central role of Fe in many redox-active enzymes of the respiratory chain, has been shown to induce the accumulation of FDH transcripts in barley roots (Suzuki et al. 1998).

To further elucidate the role of formamidase and formate dehydrogenase in white lupin's adaptation to P, N, and Fe deprivation, we are currently generating RNAi-based mutants. In addition, we have sequenced the formamidase promoter, and are using promoter::

reporter gene fusions and electrophoretic mobility shift assays to assess regulatory *cis*-acting elements of this nutrient stress-responsive gene.

Acknowledgements Funding for this project has been provided by the National Institutes of Health MBRS-Score Grant SO6 GM48135. The authors wish to thank the 2008 Functional Genomics class at California State University East Bay for their help in RT-qPCR confirmation of selected genes, and Chris Baysdorfer (Department of Biological Sciences, CSU East Bay) for critical reading of the manuscript.

References

- Bi Y, Wang R, Zhu T, Rothstein S (2007) Global transcription profiling reveals differential responses to chronic nitrogen stress and putative nitrogen regulatory components in *Arabidopsis*. *BMC Genom* 8:281
- Bradford M (1976) A rapid and sensitive method for the quantitation of microgram quantities of protein utilizing the principle of protein-dye binding. *Anal Biochem* 72:248–254
- Calderon-Vazquez C, Ibarra-Laclette E, Caballero-Perez J, Herrera-Estrella L (2008) Transcript profiling of Zea mays roots reveals gene responses to phosphate deficiency at the plant- and species-specific levels. *J Exp Bot* 59:2479–2497
- Claros MG, Vincens P (1996) Computational method to predict mitochondrially imported proteins and their targeting sequences. *Eur J Biochem* 241:779–786
- Cossins E, Chen L (1997) Foliates and one-carbon metabolism in plants and fungi. *J Phytochem* 45:437–452
- Dinkelaker B, Hengeler C and Marschner H 1995 Distribution and function of proteoid roots and other root clusters. *Bot Acta* 183–200
- Dudoit S, Yang Y, Callow M, Speed T (2002) Statistical methods for identifying differentially expressed genes in replicated cDNA microarray experiments. *Stat Sin* 12:111–140
- Emanuelsson O, Nielsen H, von Heijne G (1999) ChloroP, a neural network-based method for predicting chloroplast transit peptides and their cleavage sites. *Prot Sci* 8:978–984
- Ferber D, Khambaty F, ELY B (1988) Utilization of histidine by *Caulobacter crescentus*. *J Gen Microbiol* 134:2149
- Fournand D, Arnaud A (2001) Aliphatic and enantioselective amidases: from hydrolysis to acyl transfer activity. *J Appl Microbiol* 91:381–393
- Fraser J, Davis M, Hynes M (2001) The formamidase gene of *Aspergillus nidulans*: regulation by nitrogen metabolite repression and transcriptional interference by an overlapping upstream gene. *Genetics* 157:119–131
- Gilbert G, Knight J, Vance C, Allan D (1999) Acid phosphatase activity in phosphorus-deficient white lupin roots. *Plant Cell Environ* 22:801–810
- Gravitz N, Gleye L (1975) A photochemical side reaction that interferes with the phenolhypochlorite assay for ammonia. *Limno Oceanogr* 20:1015–1017
- Hagström J, James W, Skene K (2001) A comparison of structure, development and function in cluster roots of *Lupinus albus* L. under phosphate and iron stress. *Plant Soil* 232:81–90
- Hammond J, White P (2008) Sucrose transport in the phloem: integrating root responses to phosphorus starvation. *J Exp Bot* 59:93–109
- Horton P, Park K, Obayashi T, Fujita N, Harada H, Adams-Collier C, Nakai K (2007) WoLF PSORT: protein localization predictor. *Nucleic Acids Res* 35:W585–587
- Hynes M (1975) Amide utilization in *Aspergillus nidulans*: evidence for a third amidase enzyme. *J Gen Microbiol* 91:99–109
- Johnson J, Allan D, Vance C, Weiblen G (1996a) Root carbon dioxide fixation by phosphorus-deficient *Lupinus albus*. *Plant Physiol* 112:19–30
- Johnson J, Vance C, Allan D (1996b) Phosphorus deficiency in *Lupinus albus*. Altered lateral root development and enhanced expression of phosphoenolpyruvate carboxylase. *Plant Physiol* 112:31–41
- Kunz D, Wang C, Chen J (1994) Alternative routes of enzymic cyanide metabolism in *Pseudomonas fluorescens* NCIMB 11764. *Microbiol* 140:1705–1712
- Lamont B (2003) Structure, ecology and physiology of root clusters – a review. *Plant Soil* 248:1–19
- Liu J, Uhde-Stone C, Li A, Vance C, Allan D (2001) A phosphate transporter with enhanced expression in proteoid roots of white lupin (*Lupinus albus* L.). *Plant Soil* 237:257–266
- Liu J, Samac D, Bucciarelli B, Allan D, Vance C (2005) Signaling of phosphorus deficiency-induced gene expression in white lupin requires sugar and phloem transport. *Plant J* 41:257–268
- Lu P, Zhang F (1995) Mechanism of manganese toxicity induced by P- or Fe-deficiency in *Lupinus albus* L. *Acta Phyt Sin* 21:289–294
- Marschner H (1995) Mineral nutrition of higher plants. Academic Press Inc, San Diego
- Massonneau A, Langlade N, Léon S, Smutny J, Vogt E, Neumann G, Martinoia E (2001) Metabolic changes associated with cluster root development in white lupin (*Lupinus albus* L.): relationship between organic acid excretion, sucrose metabolism and energy status. *Planta* 213:534–542
- Miller S, Liu J, Allan D, Menzhuber C, Fedorova M, Vance C (2001) Molecular control of acid phosphatase secretion into the rhizosphere of proteoid roots from phosphorus-stressed white lupin. *Plant Physiol* 127:594–606
- Misson J, Raghothama K, Jain A, Jouhet J, Block M, Bligny R, Ortet P, Creff A, Somerville S, Rolland N, Dumas P, Nacry P, Herrera-Estrella L, Nussaume L, Thibaud M (2005) A genome-wide transcriptional analysis using *Arabidopsis thaliana* Affymetrix gene chips determined plant responses to phosphate deprivation. *Proc Natl Acad Sci USA* 102:11934–11939
- Ness S (2007) Microarray analysis: basic strategies for successful experiments. *Mol Biotech* 36:205–219
- Neumann G, Martinoia E (2002) Cluster roots – an underground adaptation for survival in extreme environments. *Trends Plant Sci* 7:162–167
- Neumann G, Römheld V (1999) Root excretion of carboxylic acids and protons in phosphorus-deficient plants. *J Plant Nutr* 211:121–130
- O'Rourke J, Nelson R, Grant D, Schmutz J, Grimwood J, Cannon S, Vance C, Graham M, Shoemaker R (2009)

- Integrating microarray analysis and the soybean genome to understand the soybeans iron deficiency response. *BMC Genom* 10:376
- Orzack S, Gladstone J (1994) Quantitative genetics of sex ratio traits in the parasitic wasp, *Nasonia vitripennis*. *Genetics* 137:211–220
- Peñaloza E, Corcuera L, Martinez J (2002) Spatial and temporal variation in citrate and malate exudation and tissue concentration as affected by P stress in roots of white lupin. *Plant Soil* 241:209–221
- Price J, Laxmi A, St Martin S, Jang J (2004) Global transcription profiling reveals multiple sugar signal transduction mechanisms in *Arabidopsis*. *Plant Cell* 16:2128–2150
- Sambrook J, Russell D (2001) Molecular cloning: a laboratory manual. CSHL press
- Sas L, Rengel Z, Tang C (2001) Excess cation uptake, and extrusion of protons and organic acid anions by *Lupinus albus* under phosphorus deficiency. *Plant Sci* 160:1191–1198
- Sas L, Rengel Z, Tang C (2002) The effect of nitrogen nutrition on cluster root formation and proton extrusion by *Lupinus albus*. *Ann Bot* 89:435–442
- Scheible W, Morcuende R, Czechowski T, Fritz C, Osuna D, Palacios-Rojas N, Schindelasch D, Thimm O, Udvardi M, Stitt M (2004) Genome-wide reprogramming of primary and secondary metabolism, protein synthesis, cellular growth processes, and the regulatory infrastructure of *Arabidopsis* in response to nitrogen I. *Plant Physiol* 136:2483–2499
- Schulze J, Temple G, Temple S, Beschow H, Vance C (2006) Nitrogen fixation by white lupin under phosphorus deficiency. *Ann Bot* 98:731–740
- Shane M, Lambers H (2005) Cluster roots: a curiosity in context. *Plant Soil* 274:101–125
- Silman N, Carver M, Jones C (1991) Directed evolution of amidase in *Methylophilus methylotrophus*; purification and properties of amidases from wild-type and mutant strains. *J Gen Microbiol* 137:169
- Simon P (2003) Q-Gene: processing quantitative real-time RT-PCR data. *Bioinformatics* 19:1439–1440
- Skouloubris S, Labigne A, De Reuse H (1997) Identification and characterization of an aliphatic amidase in *Helicobacter pylori*. *Mol Microbiol* 25:989–998
- Skouloubris S, Labigne A, De Reuse H (2001) The AmiE aliphatic amidase and AmiF formamidase of *Helicobacter pylori*: natural evolution of two enzyme paralogues. *Mol Microbiol* 40:596–609
- Suzuki K, Itai R, Nakanishi H, Nishizawa N, Yoshimura E, Mori S (1998) Formate dehydrogenase, an enzyme of anaerobic metabolism, is induced by iron deficiency in barley roots. *Plant Physiol* 116:725–732
- Thimm O, Essigmann B, Kloska S, Altmann T, Buckhout T (2001) Response of *Arabidopsis* to iron deficiency stress as revealed by microarray analysis. *Plant Physiol* 127:1030–1043
- Uhde-Stone C, Zinn K, Ramirez-Yáñez M, Li A, Vance C, Allan D (2003) Nylon filter arrays reveal differential gene expression in proteoid roots of white lupin in response to phosphorus deficiency. *Plant Physiol* 131:1064–1079
- Uhde-Stone C, Liu J, Zinn K, Allan D, Vance C (2005) Transgenic proteoid roots of white lupin: a vehicle for characterizing and silencing root genes involved in adaptation to P stress. *Plant J* 44:840–853
- Vance C (2001) Symbiotic nitrogen fixation and phosphorus acquisition. Plant nutrition in a world of declining renewable resources. *Plant Physiol* 127:390–397
- Vance CP, Uhde-Stone C, Allan DL (2003) Phosphorus acquisition and use: critical adaptations by plants for securing a nonrenewable resource. *New Phytol* 157:423–447
- Vandesompele J, De Preter K, Pattyn F, Poppe B, Van Roy N, De Paepe A, Speleman F (2002) Accurate normalization of real-time quantitative RT-PCR data by geometric averaging of multiple internal control genes. *Genome Biol* 3:0034
- Watson M, Dukes J, Abu-Median A, King D, Britton P (2007) DetectiV: visualization, normalization and significance testing for pathogen-detection microarray data. *Genome Biol* 8:R190
- Welch R, Graham R (2004) Breeding for micronutrients in staple food crops from a human nutrition perspective. *J Exp Bot* 55:353–364
- Wyborn N, Mills J, Williams S, Jones C (1996) Molecular characterisation of formamidase from *Methylophilus methylotrophus*. *Eur J Biochem* 240:314–322
- Zhou K, Yamagishi M, Osaki M, Masuda K (2008) Sugar signalling mediates cluster root formation and phosphorus starvation-induced gene expression in white lupin. *J Exp Bot* 59:2749–2756